Bone 84 (2016) 139–147

Contents lists available at ScienceDirect

Bone

journal homepage: www.elsevier.com/locate/bone

Original Full Length Article

The y6 receptor suppresses bone resorption and stimulates bone formation in mice via a suprachiasmatic nucleus relay

Ee-Cheng Khor [b,1], Ernie Yulyaningsih [a,1], Frank Driessler [b,1], Natasha Kovaĉić [b], Natalie K.Y. Wee [b], Rishikesh N. Kulkarni [b], Nicola J. Lee [a,c], Ronaldo F. Enriquez [b], Jiake Xu [d], Lei Zhang [a], Herbert Herzog [a,c,1], Paul A. Baldock [b,c,*,1]

[a] Neuroscience Division, Garvan Institute of Medical Research, 384 Victoria Street, Darlinghurst, Sydney, NSW 2010, Australia
[b] Osteoporosis and Bone Biology Division, Garvan Institute of Medical Research, 384 Victoria Street, Darlinghurst, Sydney, NSW 2010, Australia
[c] Faculty of Medicine, University of NSW, Kensington, Sydney, NSW 2052, Australia
[d] School of Pathology and Laboratory Medicine, The University of Western Australia, Crawley, WA 6009, Australia

ARTICLE INFO

Article history:
Received 24 June 2015
Revised 6 December 2015
Accepted 19 December 2015
Available online 22 December 2015

Keywords:
Neuropeptide Y
y6 receptor
Bone
Hypothalamus
Osteoblast
Osteoclast

ABSTRACT

The neuropeptide Y system is known to play an important role in the regulation of bone homeostasis and while the functions of its major receptors, Y1R and Y2R, in this process have become clearer, the contributions of other Y-receptors, like the y6 receptor (y6R), are unknown. Y6R expression is restricted to the suprachiasmatic nucleus (SCN) of the hypothalamus, an area known to regulate circadian rhythms, and the testis. Here we show that lack of y6R signalling, results in significant reduction in bone mass, but no changes in bone length. Male and female y6R knockout (KO) mice display reduced cortical and cancellous bone volume in axial and appendicular bones. Mechanistically, the reduction in cancellous bone is the result of an uncoupling of bone remodelling, leading to an increase in osteoclast surface and number, and a reduction in osteoblast number, osteoid surface, mineralizing surface and bone formation rate. y6R KO mice displayed increased numbers of osteoclast precursors and produced greater numbers of osteoclasts in RANKL-treated cultures. They also produced fewer CFU-ALP osteoblast precursors in the marrow and showed reduced mineralization in primary osteoblastic cultures, as well as reduced expression for the osteoblast lineage marker, alkaline phosphatase, in bone isolates. The almost exclusive location of y6Rs in the hypothalamus suggests a critical role of central neuronal pathways controlling this uncoupling of bone remodelling which is in line with known actions or other Y-receptors in the brain. In conclusion, y6R signalling is required for maintenance of bone mass, with loss of y6R uncoupling bone remodelling and resulting in a negative bone balance. This study expands the scope of hypothalamic regulation of bone, highlighting the importance for neural/endocrine coordination and their marked effect upon skeletal homeostasis.

1. Introduction

Bone remodelling regulates bone mass through the process of bone resorption by osteoclasts followed by bone formation by osteoblasts [1]. In addition to well established endocrine and paracrine actions, bone mass is also regulated by neural and neuropeptide mediators which have their origins in the hypothalamus [2–4]. The importance of central signalling to the maintenance of bone mass has been highlighted in recent years, with identification of an increasing number of pathways from the brain to the cells of bone, with the neuropeptide Y (NPY) family being one of the most prominent [5].

The NPY system consists of three ligands – NPY, peptide YY (PYY) and pancreatic polypeptide (PP) – which signal through 5 known G protein-coupled receptors, namely Y1, Y2, Y4, Y5 and y6 receptors (Y1R, Y2R, Y4R, Y5R, y6R). Aside from their distinct tissue expression profiles, the Y-receptors exhibit distinct binding affinities to their ligands (reviewed in [6]), with Y1R, Y2R and Y5R displaying high affinities to NPY and PYY peptides, while Y4R and y6R preferentially binding PP [7–9].

NPY and PYY have been shown to regulate bone mass in a neural and endocrine fashion, respectively [5,10,11]. Mice lacking NPY displayed increased cortical and cancellous bone mass and osteoblast activity, while hypothalamus-specific overexpression of NPY led to a significant reduction in bone mass [12–14]. Similar to the central action of NPY, restricted overexpression of NPY in osteoblasts and osteocytes in mice led to reduced cortical and cancellous bone volume and osteoblast activity

* Correspondence author at: Osteoporosis and Bone Biology Division, Garvan Institute of Medical Research, 384 Victoria Street, Darlinghurst, Sydney, NSW 2010, Australia. Tel.: +61 2 9295 8244; fax: +61 2 9295 8241.
E-mail address: p.baldock@garvan.org.au (P.A. Baldock).
[1] These authors contributed equally to this work.

http://dx.doi.org/10.1016/j.bone.2015.12.011
8756-3282/

[15]. Like NPY, PYY appears to have a negative relationship with osteoblast activity, with deletion of PYY leading to increased cancellous bone mass in association with enhanced osteoblast activity in the mouse, with opposing actions in PYY transgenic mice [16]. Lastly, based on transgenic data, elevated PP levels do not appear to play a major role in bone homeostasis [17], however, specific deletion studies of ligand or receptor have not been carried out, until now.

The actions of the NPY family of ligands on bone regulation are primarily thought to occur via Y1R and Y2R. Y1R are expressed in bone marrow stromal cells, a source of osteoprogenitor cells, as well as in osteoblasts and osteocytes [18,19]. Germline and osteoblast-specific Y1R knockout mice both demonstrate greater bone volume resulting from a greater rate of bone formation, pointing to a bone-specific role of Y1R on the modulation of bone metabolism [20,21]. Contrary to Y1R, Y2R action appears to regulate bone metabolism centrally, consistent with the lack of Y2 receptor expression in bone tissue and the observed bone phenotype of hypothalamic-specific, adult-onset Y2R deletion in mice [2]. The Y5R is expressed in bone marrow cells and has been shown to positively regulate bone marrow cell proliferation in an in vitro setting [22], but the other aspects of bone homeostasis have so far not been investigated.

The role of y6R in bone regulation is also yet to be determined. Among the Y-receptors, y6R is unique. Although it is expressed as a functional receptor in mice and rabbits [9,23–26], the y6R gene is absent from the rat [23] and only exists in a truncated version in primates, including human [9,24,27], missing the seventh transmembrane domain otherwise typical for G-protein coupled receptors. Interestingly however, unlike most 'pseudogenes' that are transcribed in very low levels [28], the human y6R mRNA is found to be highly expressed in several human tissues including the heart and skeletal muscle, as well as in the brain, gastrointestinal tissues and adrenal glands [9,23,24], indicating a potential function of this shortened gene product in humans.

We recently demonstrated that the mouse y6R is specifically expressed in the hypothalamic suprachiasmatic nucleus (SCN), specifically in neurons that co-express vasoactive intestinal peptide (VIP), a key regulator of the growth hormone axis (GH) and circadian regulation [26]. Furthermore, we identified PP as the endogenous high affinity ligand for the mouse y6R. Importantly, activation of y6R/VIP neurons in the SCN by PP increased energy expenditure and reduced feeding. As a result, inactivation of the y6R gene in the mouse led to a pronounced effect on body weight regulation, with y6R KO mice demonstrating reduced somatic growth, an increased propensity to develop age- and diet-induced obesity, and a dampened daily oscillation in circulating corticosterone and IGF-1 production [26].

Considering the critical role that the NPY system plays in the coordinated control of energy and bone homeostasis, together with the fact that the y6R is expressed in the SCN of the hypothalamus, a critical region for homeostatic regulation; we set out to identify the contributions that y6R signalling has to bone homeostasis. To achieve this goal, we utilised our y6R knockout (y6R KO) model and investigated bone mass, indices of bone turnover in vivo and in vitro, and the putative regulators of this pathway.

2. Materials and methods

2.1. Mice

All animal experiments and care were approved by the Garvan Institute/St. Vincent's Hospital Animal Experimentation Ethics Committee. Male mice were used throughout the study unless otherwise stated. y6R KO mice were generated by insertion of a selection cassette containing the lacZ and neomycin resistance (neoR) genes into the y6R coding exon, and were bred on a mixed C57BL/6–129/SvJ background [26].

2.2. Tissue collection

Mice were sacrificed by cervical dislocation followed by decapitation and hindlimbs were dissected and fixed in 4% PBS-buffered paraformaldehyde overnight at 4 °C for ex vivo phenotyping.

For RNA, following excision of the femur and tibia, and removal of the proximal and distal ends, marrow was excluded by flushing with saline, then centrifuging at 14,000 rpm for 15 s. Bones were cleaned and immediately homogenised in TRIzol reagent (Life Technologies, Grand Island, NY, USA) as described below.

2.3. Bone densitometry

Bone densitometry was performed as previously described [11]. Whole body bone mineral density (BMD) and bone mineral content (BMC) were measured with mice ventral side down (head and tail inclusion), using a dedicated mouse dual energy X-ray absorptiometer (DXA) (Lunar Piximus II, GE Medical Systems, Madison, WI), as previously described [10]. Whole femoral BMD and BMC were measured in excised left femora. Femora were DXA scanned with tibiae attached and the knee joint in flexion to 90° to ensure consistent placement and scanning of the sagittal profile.

2.4. Bone histomorphometry

After fixation and dehydration, the distal half of femurs were embedded undecalcified in methyl-methacrylate (Medim-Medizinische Diagnostik, Giessen, Germany). Sagittal 5 μm sections were stained and evaluated as previously [29]. Analysis of cancellous bone volume (BV/TV, %), trabecular thickness (Tb.Th, μm), and number (Tb.N,/mm) was carried out on modified von Kossa stained sections. To assess bone formation indices, subcutaneous (s.c.) calcein (20 mg/kg) (Sigma Chemical Company, St. Louis, USA) was given 7 and 2 days prior to collection. Mineralizing surface (MS, %) and mineral apposition rate (MAR, μm/d) were measured from unstained sections, and bone formation rate was calculated ($BFR = MS/BS * MAR$, $\mu m^2/\mu m^3/d$) [29]. Osteoid surface (OS/BS, %), osteoblast number (Ob.N/BS, %) and osteoblast number/osteoid surface (Ob.N/OS, %) were measured on sectioned stained with von Kossa, and counterstained with toluidine blue, only osteoblast directly opposed to osteoid seams were quantified [2] Bone resorption indices, osteoclast surface (Oc.S/BS, %) and number (Oc.N/BS, mm), were estimated in tartrate-resistant acid phosphatase stained sections [19]. All cancellous measurements were conducted in a sample area bordering the epiphyseal growth plate, beginning 0.25 mm proximal to the mineralization zone and extending proximally by 4.2 mm, encompassing all the cancellous bone within the cortices [2]. Cortical mineral apposition rate was measured at the posterior endosteal midshaft, extending 1000 μm proximal from the mid-femora.

2.5. Micro-computed tomography (microCT)

A Skyscan 1174 scanner and associated analysis software (Skyscan, Aartselaar, Belgium) were used to examine 3-dimensional bone structure as previously described [30]. Following fixation, bone was scanned in a plastic tube filled with 70% ethanol. A 0.5 mm aluminum filter was applied to the 50 kV X-ray source, exposure time of 3600 ms and sharpening at 40%. Distal femora were scanned at a 6.2 μm pixel resolution acquired over an angular range of 180°, with a rotation step of 0.4°. Following reconstruction, cortical bone analyses were carried out in 150 slices (0.93 mm) starting 4.5 mm proximal from the distal growth plate using CT-Analyser software (Skyscan, Aartselaar, Belgium).

2.6. Bone cell cultures

Bone cell cultures were performed following flushing of the bone marrow from femoral and tibial bones by a 23-gauge needle syringe

into complete α-MEM (10% FCS, 100 U/ml PenStrep, 1 × GlutaMax) and cultured in T-75 flasks for bone marrow mesenchymal stromal cells or with 10 ng/ml murine M-CSF for bone marrow monocyte (BMM) cultures. Non-adherent cells were discarded through media changes.

2.7. Colony forming unit — fibroblast (CFU-F) assay

Fresh bone marrow extracted from y6R KO mouse tibia and femur were plated at cell densities of 4×10^5 and 8×10^5 in 6-well plates in complete αMEM with 50 μg/ml ascorbic acid and 10 nM dexamethasone. Media was changed every three days for 18 days then washed in PBS before fixation in cold 90% ethanol for 10 min. The colonies were stained for Alkaline Phosphatase (ALP) [31]. Colonies were counted in ImageJ software (National Institutes of Health, Bethesda, MD, USA) from scanned images processed with threshold and Gaussian blur (2 pixel radius) in Adobe Photoshop (Adobe, San Francisco, CA, USA).

2.8. Osteoblast differentiation from bone marrow stromal cells (BMSCs)

Bone marrow was extracted from WT and y6R KO hind limb bones and cultured in αMEM for plastic adherent BMSC. BMSCs were seeded at 6×10^4 cells/well in 24-well plates and cultured with 50 μg/ml ascorbic acid, 10 nM dexamethasone and 5 mM β-glycerophosphate for 14 days. The cultures were fixed in 4% paraformaldehyde for 10 min and stained with Alizarin Red staining solution. Mineralization surface was quantified through ImageJ particle analysis of scanned images.

2.9. Osteoclast differentiation from BMM

BMM cells were seeded at a density of 6×10^3 cells per well in 96-well plates and cultured in 10 ng/ml M-CSF (Peprotech, Japan) with the indicated concentrations of murine sRANKL (Peprotech, Japan) for 5 days. A RANKL time course was performed at the allocated time points (0, 2, 3, 4, 5 days) with 50 ng/ml sRANKL. Total RNA was isolated from cells after 3 days in culture using Direct-zol™ RNA MiniPrep as per the manufacturer's instructions (Zymo Research Corporation, CA, USA) and Reverse Transcription was performed using the Superscript III First-Strand Synthesis System (Life Technologies, Grand Island, NY, USA). Real-time PCR reactions for GAPDH, cathepsin K, NFATc1 and tartrate-resistant acid phosphatase (TRAP) were performed using the Power SYBR® Green PCR Master Mix (Applied Biosystems) in an ABI Prism 7900 HT sequence detector (Applied Biosystems). Primers used were as follows: NFATc1 (sense: 5′-AGCCCATCCTTGCCTGCCT-3′, antisense: 5′-CCGTGTAGCTGCACAATGGGG-3′), TRAP (sense: 5′-GGGGAC AATTTCTACTTCACTGG-3′, antisense: 5′-GCAAACGGTAGTAAGGGCTG-3′), CATHEPSIN K (sense: 5′-GGCCAGTGTGGTTCCTGTT-3′, antisense: 5′-CAGTGGTCATATAGCCGCCTC-3′), and GAPDH (sense: 5′-GCATCTCC CTCACAATTTCCA-3′, antisense: 5′-GTGCAGCGAACTTTATTGATGG-3′).

2.10. Analysis of gene expression in bone tissue

RNA was isolated from cleaned tibiae using TRIzol® reagent as per the manufacturer's instructions. RNA was reverse transcribed with hexamer primers using the Invitrogen Superscript II First strand synthesis kit (Life Technologies, Grand Island, NY, USA) according to manufacturer's instructions. qPCR was performed with the TaqMan gene expression assay (Life Technologies, Grand Island, NY, USA) according to manufacturer's instructions. y6R expression was evaluated as previously [26]. TaqMan gene expression assays for RANKL, OPG and ACTB as well as RUNX-2 and ALP were used with TaqMan gene expression master mix. Primer sequences for osterix, GAPDH are as follows: OSTERIX (sense: 5′-AGAGGTTCACTCGCTCTGACGA-3′, antisense: 5′-TTGCTCAAGTGGTCGCTTCTG-3′), GAPDH (sense: 5′-GCATCTCCCTCA CAATTTCCA-3′, antisense: 5′-GTGCAGCGAACTTTA TTGATGG-3′). The absolute quantification method was used with a standard curve created from pooled cDNA samples serial diluted 1:2. The PCR reactions were done in triplicate in 384-well plates at 10 μl reaction volumes with sample cDNA quantity of 400 ng per reaction. Real-time polymerase chain reaction reactions were performed using the TaqMan Universal PCR master mix in an ABI Prism 7900 HT sequence detector (Life Technologies, Grand Island, NY, USA).

2.11. Flow cytometry

The BD Biosciences protocol was used to immunostain mouse bone marrow cells. In brief, bone marrow cells were extracted from mice hind limbs. Red blood cells (RBCs) were lysed in ammonium chloride lysis buffer (0.15 M NH_4Cl, 10 mM Tris–HCl, 0.1 mM EDTA) and the cells were resuspended in ice cold wash buffer (2% FBS in PBS). Bone marrow cell suspensions (10^6 cells) were incubated with CD45R-FITC (RA3-6B2), CD3-FITC (145-2C11), CD11b-PE (clone), CD115-APC (AFS98), CD117-Pacific Blue (2B8), and RANK-Biotin (R12-31) antibodies for 30 min in the dark. RANK-Biotin stained cells were washed and stained with streptavidin-PECy7. The cells were washed twice (~10^6 cells) and transferred to flow cytometer tubes containing cold wash buffer with DAPI. The BD LSR-SORPII flow cytometer (BD Biosciences, San Jose, CA, USA) was used for analysis. Dead cells stained positive for DAPI were excluded.

2.12. Statistical analysis

Data are expressed as means ± standard error (SEM). Differences between genotypes were assessed by two-tailed Student's t-test using GraphPad Prism 5 (Version 5.0a, GraphPad Software, Inc., La Jolla, CA, USA). For all statistical analyses, p values below 0.05 were considered statistically significant.

3. Results

3.1. Lack of y6R gene expression in bone cells

Since y6R expression had only been described in the brain and testis, we first sought to establish the possibility of a direct y6R control of bone homeostasis by examining its expression in bone cells. As described previously [26], deletion of the y6R in this mouse model is achieved by insertion of the lacZ gene, thereby allowing detection of its normal tissue distribution via ß-gal staining. Utilising the introduced lacZ gene, we investigated the expression pattern of y6R in a variety of peripheral tissues and throughout the brain. Only a subset of neurons within the hypothalamic suprachiasmatic nucleus (SCN) showed staining for β-gal, with no staining in any other area of the brain, bone sections or the other peripheral tissues examined, except testes [26]. Furthermore, semi-quantitative PCR analysis showed y6R mRNA expression in the hypothalamus and testis as previously reported, but not in various bone components, including bone marrow, bone marrow-derived monocytes (BMM), osteoclasts, bone marrow stromal cells (BMSCs), and osteoblasts (Fig. 1). These findings suggest that any effect of y6R signalling on bone regulation must occur indirectly, most likely via the hypothalamic SCN where y6R are expressed at high levels [26].

3.2. Lack of y6R signalling leads to reduced bone mass in mice

We next investigated the contribution of y6R signalling to bone regulation by examining a germline y6R KO model (Fig. 2A). Contrary to the observed increase in bone density and mass in the Y1R KO and Y2R KO mice, DXA analysis of 16-week-old male mice showed a significant reduction in whole body BMD and BMC in the absence of y6R (Fig. 2B). DXA analysis of isolated femurs also revealed a marked reduction in BMD and BMC in y6R KO compared to wildtype controls (Fig. 2C). Compared to their wildtype counterparts, microCT analysis of the distal femoral metaphysis revealed reduced cancellous bone

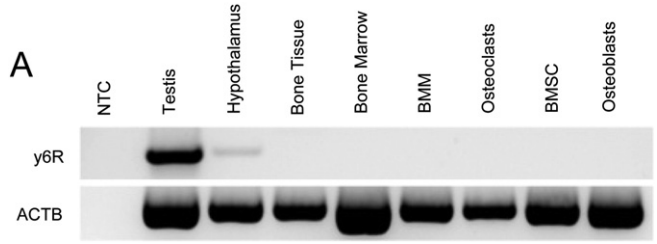

Fig. 1. y6R gene expression. (A) Semi-quantitative PCR detects the expression of y6R in the mouse testis and hypothalamus. There is no evidence of y6R expression in whole bone tissue, osteoclast osteoblast cell lineages or their precursors, bone marrow monocytes (BMM) and bone mesenchymal stem cells (BMSC), respectively. Beta actin (ACTB) was used as a house keeping control. NTC, no reverse transcriptase control (testis RNA).

volume in y6R KO mice, in association with lower trabecular number without any change in trabecular thickness (Fig. 2D). Femur length is not significantly different between y6R KO and control mice, however, cross-sectional cortical area, cortical thickness and periosteal perimeter, but not endosteal perimeter, were reduced in y6R KO femurs compared to those of controls (Fig. 2E). These changes were evident in both male and female y6R KO mice (Supplementary Fig. 1), suggesting a generalised effect on bone mass caused by the absence of y6R signalling in mice. Further, analysis of the axial skeleton shows that deletion of y6R in mice led to a pronounced reduction in the cancellous bone volume, trabecular number and thickness in the L3 vertebral body (Fig. 2F). Also consistent with the femoral changes of y6R KO mice, we observe a significant reduction in the vertebral cortical volume and thickness in these mice, without any change to vertebral length (Fig. 2G). These data identify y6R signalling as a novel central pathway to bone.

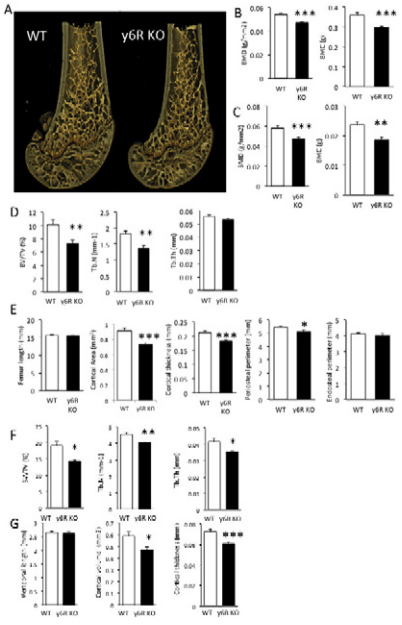

Fig. 2. Reduced bone mass in adult y6R-deficient mice. (A) Representative microCT images of 16 week old male WT and y6R KO mice. (B) DXA analysis of 16 week old male WT and y6R KO mice showing reduced whole body BMD and BMC and reduced (C) femoral DXA BMD and BMC in 16 week old male y6R KO compared to WT. (D) MicroCT analysis showing reduced bone volume in the distal femoral metaphysis, (E) mid-femoral cortical bone, (F) L3 vertebral cancellous and (G) L3 vertebral cortical bone of y6R KO mice. Mean + SEM n = 7–18. *p < 0.05, **p < 0.01, ***p < 0.001.

3.3. Reduced bone mass in y6R KO mice is associated with increased osteoclast number

In order to investigate the underlying mechanism of the reduced bone mass in these mice, bone cell activities were analysed by histomorphometry in the distal femoral metaphysis of 16-week-old male wildtype and y6R KO mice. As with the, microCT analysis, cancellous bone volume and trabecular number were reduced in y6R KO relative to control mice (Fig. 3A). Consistent with reduced bone volume, we found a greater osteoclast number (Oc.N/BS) and osteoclast surface (Oc.S/BS) in y6R KO compared to WT (Fig. 3B), suggesting an increase in bone resorption. Interestingly, the bone formation indices, mineral apposition rate (MAR), mineralizing surface (MS/BS) and bone formation rate (BFR), were unchanged between y6R KO and WT, suggesting uncoupled remodelling favouring bone resorption. Osteoid surface (OS/BS) was significantly reduced in y6R KO mice, however despite greater osteoclast number, osteoblast number (Ob.N/BS) and osteoblast number per osteoid surface (OB.N/OS) were not different between genotypes (Fig. 3B). These findings identify signalling through y6R as the first NPY-family pathway to repress bone resorption and increase bone mass.

To further investigate the role of osteoclasts in the observed phenotype, gene expression of RANKL and OPG was examined. Interestingly, the ratio of RANKL:OPG mRNA was not significantly different between y6R KO and WT mice (Fig. 3C), suggesting the potential for an osteoclast-intrinsic change. To determine this, we tested the osteoclastogenic potential of bone marrow-derived cells from y6R KO and WT mice. In vitro osteoclast cultures from y6R KO bone marrow monocytes (BMMs) showed a significant increase in $TRAP^+$ multinucleated cells 5 days after RANKL treatment (50 ng/ml) compared to WT controls (Fig. 3D). BMMs from y6R KO mice also formed more $TRAP^+$ multinucleated cells at suboptimal doses of RANKL relative to those of wildtype animals (Fig. 3E). Consistent with greater $TRAP^+$ multinucleated cell number in culture, NFATc1 expression was elevated 2-fold at 24 h in y6R KO BMM cultures. The mRNA expression levels of the osteoclastic genes cathepsin K, NFATc1 and TRAP were not significantly different between wildtype and y6 deficient BMMs 3 days after RANKL treatment at 20 ng/ml (Supplementary Fig. 2). To test whether greater NFATc1 expression may result from greater immature osteoclastic cells in y6R KO marrow, flow cytometry analysis of bone marrow from y6R KO and WT mice identified a significant increase in osteoclast progenitor ($CD11b^{low}CD3^-CD45R^-CD115^+CD117^{high}$) cell population in y6R KO marrow (Fig. 3F). There was also a significant increase in pre-osteoclast ($RANK^+CD115^+$(c-fms)) cells (Fig. 3G). Taken together, these results indicate that in the absence of y6R, mice have increased osteoclastogenic potential associated with increased osteoclast progenitor and pre-osteoclastic cell populations.

3.4. Reduced bone mass in y6R KO mice is associated with suppression of bone formation

The observed increase in osteoclast parameters without any change in osteoblast parameters indicates an uncoupling of bone remodelling in y6R KO mice. The lack of an osteoblastic response to the increased osteoclastic activity suggests a potential inhibition of osteoblastogenesis in y6R KO mice. In order to further examine bone remodelling in y6R KO mice, we investigated the bones of 24-week-old mice (Fig. 4A). Consistent with the bone phenotype of 16-week-old y6R KO mice, analysis showed a marked reduction in the femoral BMD and BMC, as well as cortical area and cortical thickness of 24-week-old y6R KO compared to age-matched WT controls (Fig. 4B). MicroCT demonstrated a significant reduction in cancellous bone volume associated with reduced trabecular number and thickness (Fig. 4A, C). Osteoclast surface and osteoclast numbers were again greater in y6R KO mice relative to WT controls at 24 weeks of age. In addition, mineralizing surface and bone formation rate osteoid surface (OS/BS), osteoblast number (Ob.N/BS)

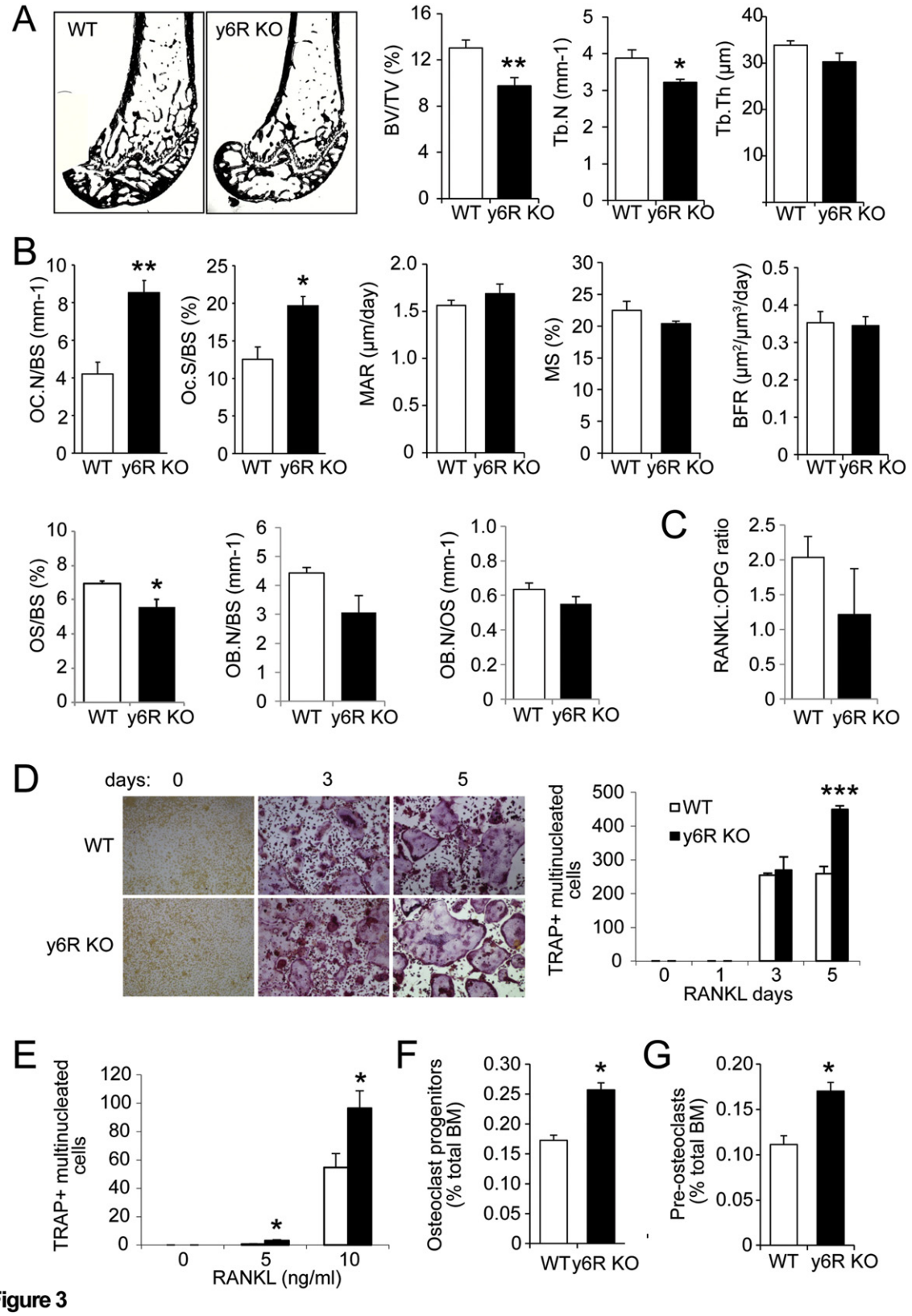

Figure 3

Fig. 3. Elevated bone resorption in y6R deficient mice. (A) Representative sagittal sections and cancellous microstructure of distal femur of 16 week old male WT and y6R KO mice demonstrating reductions in cancellous bone volume, trabecular number and trabecular thickness evident following histomorphometric analysis. (B) Bone cell activity in the distal femoral metaphysis, revealed elevated osteoclast number and surface, with no difference in dynamic bone formation indices, but a reduction in osteoid surface, with no change in osteoblast number. (C) No difference in RANKL:OPG gene expression in bone isolates from WT and y6R KO mice. (D) Greater RANKL stimulated osteoclast production from bone marrow of y6R KO compared to WT mice. (E) Greater osteoclast production from bone marrow of y6R KO mice using sub-optimal RANKL doses. (F) Greater osteoclast progenitor and (G) pre-osteoclast numbers in y6R KO marrow compared to WT. Mean + SEM n = 5–13. *$p < 0.05$, **$p < 0.01$, ***$p < 0.001$.

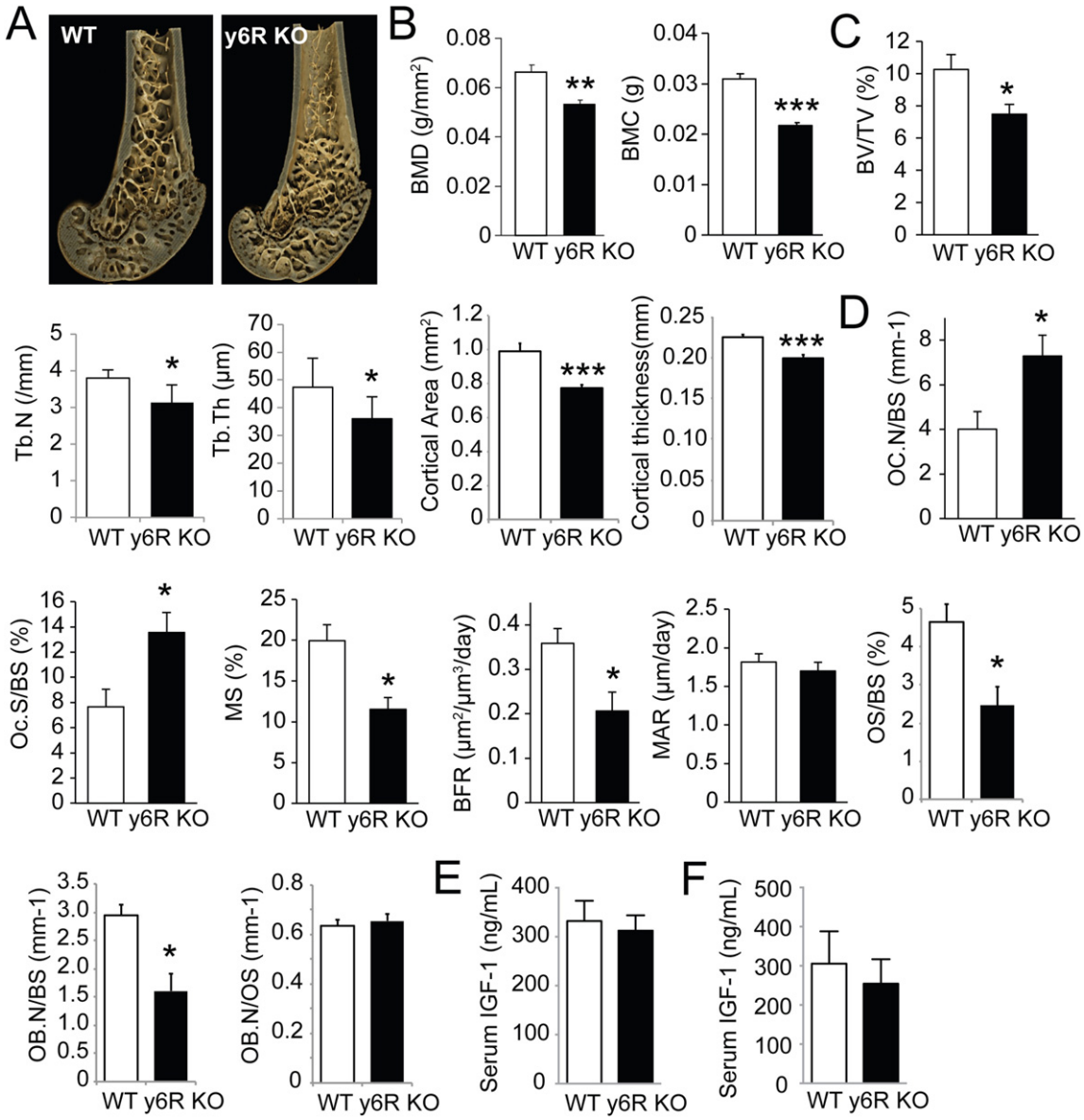

Fig. 4. Reduced bone mass and formation in aged y6R-deficient mice. (A) Representative microCT images of 24-week-old male WT and y6R KO mice, demonstrating continued loss of bone in y6R KO mice. (B) DXA analysis of femoral BMD and BMC and (C) microCT confirmation of reduced bone mass and microstructural changes in the distal femoral metaphysis and mid femoral cortical bone. (D) Bone cell activity in the distal femoral metaphysis demonstrates both increased resorption and reduced bone formation indices in y6R KO. No alteration in serum IGF-1 levels in non-fasted (E) or fasted (F) 24 week old y6R KO mice.

but not osteoblast number per osteoid surface (OB.N/OS) were of y6R KO mice were significantly reduced confirming the osteoblastic deficit (Fig. 4D). Together these findings demonstrate a dysregulation of both osteoclast and osteoblast activities in mice that lack signalling through the y6R.

Alterations in IGF-1 signalling have been shown to affect bone remodelling and we have previously shown that serum IGF-1 is significantly lower in 16 week old y6R KO mice, in association with a reduced Ghrh expression in the hypothalamus [26]. In order to determine whether the bone phenotype of y6R KO mice is being driven by alterations in IGF-1, we also measured serum IGF-1 levels in 24 week old mice. We observed a similar significant reduction in IGF-1 levels in fasted 16 week old y6R KO mice compared to control as we have published previously ([26] and data not shown). However, as shown in Fig. 4F, IGF-1 levels were unaltered in 24 week old y6R KO mice compared to controls in both the fasted and non-fasted states. Considering that the effect of y6R deletion on osteoclastogenesis is more prominent in the older animals, the lack of significant changes of IGF-1 in these mice suggests that IGF-1 may not play a major role in this process.

3.5. Deficits in osteoblast differentiation and mineralization in bone marrow of y6R KO mice

The reduction in mineralizing surface and inability to maintain coupling in the bones of y6R KO mice suggest a reduction in osteoblast proliferation. In order to investigate osteoblast differentiation and mineralization, a CFU-Ob assay was performed to determine the osteoblast proliferative potential of bone marrow cells derived from y6R KO mice. There was a significant reduction in alkaline phosphatase positive (ALP^+) CFU-Ob colonies in y6R KO bone marrow compared to that of WT mice (Fig. 5A). Mineralization of 14 day bone marrow stromal cell (BMSC) cultures was also reduced in y6R KO cells (Fig. 5A). Gene expression in bone isolates displayed a significant decrease in alkaline phosphatase, a similar trend in osterix with no change in the late marker

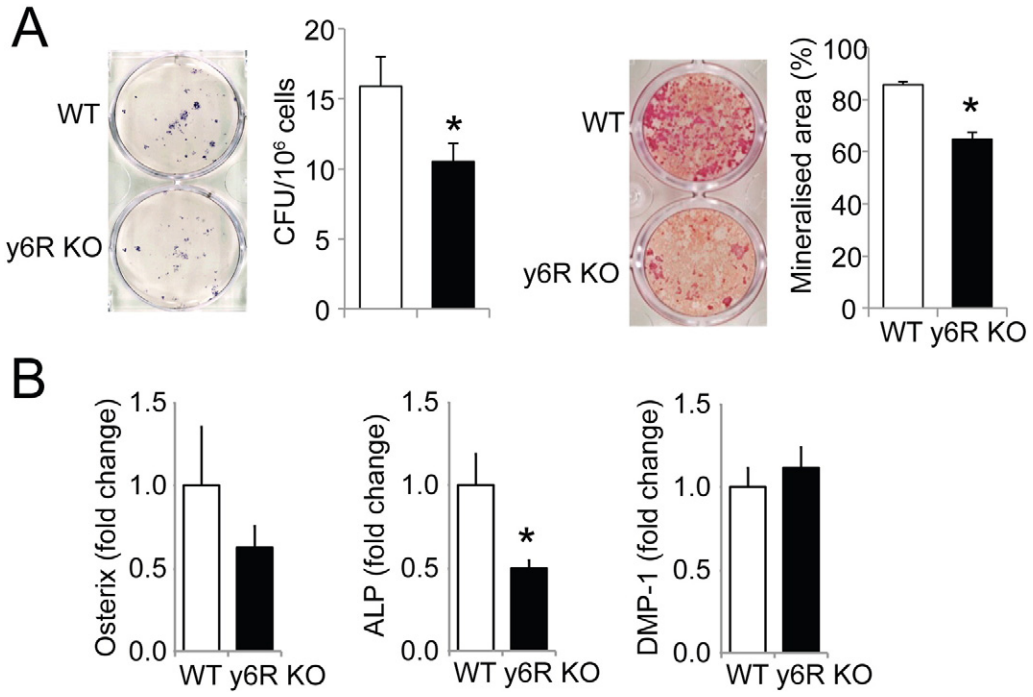

Fig. 5. Deficits in osteoblast differentiation and mineralization in bone marrow of y6R KO mice. (A) ALP^{+} CFU-Ob and mineralized nodule area reduced in cells from y6R KO marrow. (B) Expression of osteoblast markers osterix, ALP and DMP-1 in y6R KO and WT bone isolates.

DMP-1 (Fig. 5B). These findings of reduced osteoblast differentiation and activity, and reduced mineralizing surface in vivo, are consistent with an osteoblast defect in y6R KO mice. This inhibition of bone formation further reinforces the unique nature of y6R signalling to bone, being the opposite of the previously described Y1 and Y2 receptor null models [2,20,21].

4. Discussion

In this study we demonstrate that signalling through the y6 receptor in mice is critical for maintaining normal bone homeostasis, with lack of y6R in mice leading to a significant and generalised reduction in bone mass. This reduction does not appear to involve developmental changes, as bone length is not significantly altered. Rather, the bone loss is the result of uncoupled bone remodelling involving increased osteoclastogenesis and reduced osteoblastogenesis, evident in both genders and in adult and aged mice. This is manifested as a remodelling imbalance, producing significant reductions in cancellous and cortical bone parameters in both long bones and vertebrae. Importantly, y6R is undetectable in whole bone, bone cells or their precursors, but is strongly expressed in the hypothalamus, and with an expression profile unique to previously defined Y-receptors. Thus, despite the absence of evidence for a functional Y6R in humans, it is clearly important to murine homeostasis, and must be considered when evaluating murine models, which modulate the NPY system. The lack of detectable expression of y6R and lacZ in bone tissue or bone cells suggests an indirect response. The two major expression sites are the SCN of the hypothalamus and testis with y6R in the testis are less likely to play a critical role since the lack of y6R affected male and female mice in the same way, though minor contributions to the male phenotype cannot be completely excluded. Considering that the only other area with high levels of y6R expression is the SCN identifies this population of neurons as the prime candidates that mediate y6R signalling controlled processes. The SCN is the major site of circadian regulation, and has received substantial interest in recent years. Consistent with the phenotype in the y6R KO mice, bone is also a tissue that displays circadian patterns [32]. Disruption of circadian rhythm by day length modification or surgical pinealectomy has been shown to alter bone remodelling. The identification of neural output from the SCN in response to activation of y6R signalling represents a new aspect of circadian signalling to bone. Moreover, combined with the metabolic changes previously outlined in this model [26]; signalling through y6R in the SCN represents a powerful mediator of homeostatic changes in both energy and bone homeostasis, two processes that are increasingly appreciated to be linked, particularly by central neuropeptide pathways [33].

Previous studies of central NPY signalling to bone have focused upon the arcuate nucleus, a region pivotal to metabolic homeostasis, and have contributed to our growing appreciation of neural regulation of bone, and the links between energy and bone homeostasis. Similarly, the current study also focuses upon a region with wide ranging regulatory influence, the SCN; a master regulator of circadian rhythms, establishing y6R signalling as a novel mechanism regulating bone homeostasis. However, there are important differences between the arcuate and SCN pathways. The pathway from the arcuate nucleus is signalled by Y2R and specifically suppresses the activity of osteoblasts, through regulation of efferent neural outflow, but does not alter osteoblast proliferation or bone resorption. The y6R pathway displays a more complex, wide ranging response. Data for y6R KO mice define a pathway regulating both osteoclastic and osteoblastic proliferation, and doing so in opposing directions: Identifying y6 signalling as capable of simultaneously repressing bone resorption and stimulating bone formation. Moreover, the y6R pathway also regulates metabolic activity [26]. The leptin-deficient ob/ob mouse is another model, which displays metabolic responses as well as alteration of both bone resorption and formation. While leptin deficiency results in a number of endocrine changes, including greater corticosterone and reduced IGF-1 [36], the alteration of remodelling in cancellous bone in ob/ob results predominantly from a combination of reduced sympathetic outflow and central cocaine- and amphetamine regulated transcript (CART) expression. In addition, the ob/ob model has reduced cortical bone mass and formation, driven by elevated NPY expression, consistent with the starvation signals (and perceived lack of adipose tissue/negative energy balance) triggered by the lack of leptin signalling in the hypothalamus [37]. Interestingly, the y6R KO model also demonstrates a coordinated response

between bone and energy homeostasis. y6R KO mice have reduced bone mass and a negative bone balance which is coincident with a negative energy balance and reduced body weight and lean mass [26]. Also similar to ob/ob, y6R KO display a number of endocrine change, also affecting corticosterone and IGF-1. Serum IGF-1 is lower in young adult but not aged y6R KO mice, in association with a reduced Ghrh expression in the hypothalamus. In addition, corticosterone diurnal rhythmicity is lost in y6R KO mice, with no increase during the light hours, leading to chronically reduced levels [26]. While these changes may influence body mass, they do not appear to be crucial to the bone phenotype, particularly in aged mice. In this manner, the y6R represents a novel central pathway to bone that is capable of a non-coupled increase in bone mass, while also increasing body weight and lean mass.

Although functional characterization of the mouse y6R reveals critical roles of this receptor in the regulation of energy metabolism [26] and bone, little is known of its function in humans. Previous studies reported a frame-shift mutation that was introduced early in primate evolution, leading to a premature stop codon [23,24,27]. Interestingly, the human Y6R transcript is found abundantly in several tissues, particularly in the heart and skeletal muscle [9,23,24], giving rise to speculation that the product of the Y6R gene, either on a transcript or protein level, may possess some function. Indeed, truncated GPCRs with less than 7 transmembrane domains have previously been reported to play important roles by binding to related GPCRs to exert a dominant negative effect or to generate novel pharmacology [38]. Apart from acting as binding partners, some truncated GPCRs appear to retain functional activities such as a 6-transmembrane-domain μ-opioid receptor and a 5-transmembrane-domain somatostatin receptor, both of which exhibit altered pharmacology compared to their full-length counterparts and retain functional activities [39,40]. Alternatively, the functions mediated through Y6 signalling in mice could have been taken over by another Y-receptor in humans, like the Y4 receptor to which PP has also high affinity. Further studies are required to determine the exact function of the human Y6R transcript and the possible shift towards Y4 signalling by PP.

The NPY system is complex, involving 3 ligands and multiple receptors, 5 in the mouse, including y6R. A fundamental function of this system is to regulate energy homeostasis, and coordinate the conservation of energy throughout the body during periods of negative energy balance. In recent years, it has become apparent that skeletal activity is a component of the energy conservation system, and is under powerful control by the NPY system. Consistent with this activity, NPY signalling through Y2R in the arcuate nucleus reduces cortical bone mass in leptin deficient mice, with loss of Y2R completely correcting the effects of leptin deficiency on cortical bone. However, Y2R had minor effects upon metabolic responses in ob/ob [36]. y6R provide a novel and powerful addition to this system, with loss of function reducing bone mass, as well as body weight and lean mass. Thus y6R function in opposition to Y2R, as they promote lean and bone mass acquisition. As such, it is a rare factor capable of both anabolic and anti-catabolic actions, highlighting the potential therapeutic benefit of central signalling to bone.

Supplementary data to this article can be found online at http://dx.doi.org/10.1016/j.bone.2015.12.011.

Acknowledgements

This study was supported by the NHMRC of Australia project grant #1028887. HH was supported by a Senior Research Fellowship from the NHMRC #101973.

References

[1] R. Baron, Anatomy and ultrastructure of bone, in: M.F. Favus (Ed.), Primer on The Metabolic Bone Diseases and Disorders of Mineral Metabolism, fourth ed.Lippincott Williams and Wilkins, Philadelphia, PA 1999, pp. 3–10.
[2] P.A. Baldock, A. Sainsbury, M. Couzens, R.F. Enriquez, G.P. Thomas, E.M. Gardiner, H. Herzog, Hypothalamic Y2 receptors regulate bone formation, J. Clin. Invest. 109 (2002) 915–921.
[3] P. Ducy, M. Amling, S. Takeda, M. Priemel, A.F. Schilling, F.T. Beil, J. Shen, C. Vinson, J.M. Rueger, G. Karsenty, Leptin inhibits bone formation through a hypothalamic relay: a central control of bone mass, Cell 100 (2000) 197–207.
[4] I.P. Wong, A. Zengin, H. Herzog, P.A. Baldock, Central regulation of bone mass, Semin. Cell Dev. Biol. 19 (2008) 452–458.
[5] E.C. Khor, P. Baldock, The NPY system and its neural and neuroendocrine regulation of bone, Curr. Osteoporos. Rep. 10 (2012) 160–168.
[6] E. Yulyaningsih, L. Zhang, H. Herzog, A. Sainsbury, NPY receptors as potential targets for anti-obesity drug development, Br. J. Pharmacol. 163 (2011) 1170–1202.
[7] A.G. Blomqvist, H. Herzog, Y-receptor subtypes—how many more? Trends Neurosci. 20 (1997) 294–298.
[8] E.L. Hill, R. Elde, Distribution of CGRP-, VIP-, D beta H-, SP-, and NPY-immunoreactive nerves in the periosteum of the rat, Cell Tissue Res. 264 (1991) 469–480.
[9] P. Gregor, Y. Feng, L.B. DeCarr, L.J. Cornfield, M.L. McCaleb, Molecular characterization of a second mouse pancreatic polypeptide receptor and its inactivated human homologue, J. Biol. Chem. 271 (1996) 27776–27781.
[10] P.A. Baldock, N.J. Lee, F. Driessler, S. Lin, S. Allison, B. Stehrer, E.J. Lin, L. Zhang, R.F. Enriquez, I.P. Wong, M.M. McDonald, M. During, D.D. Pierroz, K. Slack, Y.C. Shi, E. Yulyaningsih, A. Aljanova, D.G. Little, S.L. Ferrari, A. Sainsbury, J.A. Eisman, H. Herzog, Neuropeptide Y knockout mice reveal a central role of NPY in the coordination of bone mass to body weight, PLoS One 4 (2009), e8415.
[11] K.E. Wortley, K. Garcia, H. Okamoto, K. Thabet, K.D. Anderson, V. Shen, J.P. Herman, D. Valenzuela, G.D. Yancopoulos, M.H. Tschop, A. Murphy, M.W. Sleeman, Peptide YY regulates bone turnover in rodents, Gastroenterology 133 (2007) 1534–1543.
[12] P.A. Baldock, S. Allison, F.-M.D. MM, M.D.M. Fau, A. Sainsbury, A. Sainsbury, R.F. Fau - Enriquez, E.R. Fau, D.G. Little, L.D.F. Eisman, E. JA, E.M. Ja Fau - Gardiner, G.E. Fau, H. Herzog, H. Herzog, Hypothalamic regulation of cortical bone mass: opposing activity of Y2 receptor and leptin pathways, J. Bone Miner. Res. (2006).
[13] P.A. Baldock, A. Sainsbury, S. Allison, E.J. Lin, M. Couzens, D. Boey, R. Enriquez, M. During, H. Herzog, E.M. Gardiner, Hypothalamic control of bone formation: distinct actions of leptin and y2 receptor pathways, J. Bone Miner. Res. 20 (2005) 1851–1857.
[14] N.J. Lee, K.L. Doyle, A. Sainsbury, R.F. Enriquez, Y.J. Hort, S.J. Riepler, P.A. Baldock, H. Herzog, Critical role for Y1 receptors in mesenchymal progenitor cell differentiation and osteoblast activity, J. Bone Miner. Res. 25 (2010) 1736–1747.
[15] I. Matic, B.G. Matthews, T. Kizivat, J.C. Igwe, I. Marijanovic, S.T. Ruohonen, E. Savontaus, D.J. Adams, I. Kalajzic, Bone-specific overexpression of NPY modulates osteogenesis, J. Musculoskelet. Neuronal Interact. 12 (2012) 209–218.
[16] I.P. Wong, F. Driessler, E.C. Khor, Y.C. Shi, B. Hormer, A.D. Nguyen, R.F. Enriquez, J.A. Eisman, A. Sainsbury, H. Herzog, P.A. Baldock, Peptide YY regulates bone remodeling in mice: a link between gut and skeletal biology, PLoS One 7 (2012), e40038.
[17] A. Sainsbury, P.A. Baldock, C. Schwarzer, N. Ueno, R.F. Enriquez, M. Couzens, A. Inui, H. Herzog, E.M. Gardiner, Synergistic effects of Y2 and Y4 receptors on adiposity and bone mass revealed in double knockout mice, Mol. Cell. Biol. 23 (2003) 5225–5233.
[18] J.C. Igwe, X. Jiang, F. Paic, L. Ma, D.J. Adams, P.A. Baldock, C.C. Pilbeam, I. Kalajzic, Neuropeptide Y is expressed by osteocytes and can inhibit osteoblastic activity, J. Cell. Biochem. 108 (2009) 621–630.
[19] P. Lundberg, C. Koskinen, P.A. Baldock, H. Lothgren, A. Stenberg, U.H. Lerner, P.A. Oldenborg, Osteoclast formation is strongly reduced both in vivo and in vitro in the absence of CD47/SIRPalpha-interaction, Biochem. Biophys. Res. Commun. 352 (2007) 444–448.
[20] P.A. Baldock, S.J. Allison, P. Lundberg, N.J. Lee, K. Slack, E.J. Lin, R.F. Enriquez, M.M. McDonald, L. Zhang, M.J. During, D.G. Little, J.A. Eisman, E.M. Gardiner, E. Yulyaningsih, S. Lin, A. Sainsbury, H. Herzog, Novel role of Y1 receptors in the coordinated regulation of bone and energy homeostasis, J. Biol. Chem. 282 (2007) 19092–19102.
[21] N.J. Lee, A.D. Nguyen, R.F. Enriquez, K.L. Doyle, A. Sainsbury, P.A. Baldock, H. Herzog, Osteoblast specific Y1 receptor deletion enhances bone mass, Bone 48 (2011) 461–467.
[22] K. Igura, H. Haider, R.P. Ahmed, S. Sheriff, M. Ashraf, Neuropeptide y and neuropeptide y y5 receptor interaction restores impaired growth potential of aging bone marrow stromal cells, Rejuvenation Res. 14 (2011) 393–403.
[23] A.M. Burkhoff, D.L. Linemeyer, J.A. Salon, Distribution of a novel hypothalamic neuropeptide Y receptor gene and its absence in rat, Mol. Brain Res. 53 (1998) 311–316.
[24] M. Matsumoto, T. Nomura, K. Momose, Y. Ikeda, Y. Kondou, H. Akiho, J. Togami, Y. Kimura, M. Okada, T. Yamaguchi, Inactivation of a novel neuropeptide Y/peptide YY receptor gene in primate species, J. Biol. Chem. 271 (1996) 27217–27220.
[25] D.H. Weinberg, D.J.S. Sirinathsinghji, C.P. Tan, L.L. Shiao, N. Morin, M.R. Rigby, R.H. Heavens, D.R. Rapoport, M.L. Bayne, M.A. Cascieri, C.D. Strader, D.L. Linemeyer, D.J. MacNeil, Cloning and expression of a novel neuropeptide Y receptor, J. Biol. Chem. 271 (1996) 16435–16438.
[26] E. Yulyaningsih, K. Loh, S. Lin, J. Lau, L. Zhang, Y. Shi, B.A. Berning, R. Enriquez, F. Driessler, L. Macia, E.C. Khor, Y. Qi, P. Baldock, A. Sainsbury, H. Herzog, Pancreatic polypeptide controls energy homeostasis via Npy6r signaling in the suprachiasmatic nucleus in mice, Cell Metab. 19 (2014) 58–72.
[27] P.M. Rose, J.S. Lynch, S.T. Frazier, S.M. Fisher, W. Chung, P. Battaglino, Z. Fathi, R. Leibel, P. Fernandes, Molecular genetic analysis of a human neuropeptide Y receptor. The human homolog of the murine "Y5" receptor may be a pseudogene, J. Biol. Chem. 272 (1997) 3622–3627.
[28] D. Zheng, A. Frankish, R. Baertsch, P. Kapranov, A. Reymond, S.W. Choo, Y. Lu, F. Denoeud, S.E. Antonarakis, M. Snyder, Y. Ruan, C.L. Wei, T.R. Gingeras, R. Guigo, J. Harrow, M.B. Gerstein, Pseudogenes in the ENCODE regions: consensus annotation, analysis of transcription, and evolution, Genome Res. 17 (2007) 839–851.

[29] S.J. Allison, P. Baldock, A. Sainsbury, R. Enriquez, N.J. Lee, E.J. Lin, M. Klugmann, M. During, J.A. Eisman, M. Li, L.C. Pan, H. Herzog, E.M. Gardiner, Conditional deletion of hypothalamic Y2 receptors reverts gonadectomy-induced bone loss in adult mice, J. Biol. Chem. 281 (2006) 23436–23444.
[30] Y.C. Shi, S. Lin, I.P. Wong, P.A. Baldock, A. Aljanova, R.F. Enriquez, L. Castillo, N.F. Mitchell, J.M. Ye, L. Zhang, L. Macia, E. Yulyaningsih, A.D. Nguyen, S.J. Riepler, H. Herzog, A. Sainsbury, NPY neuron-specific Y2 receptors regulate adipose tissue and trabecular bone but not cortical bone homeostasis in mice, PLoS One 5 (2010), e11361.
[31] C.G. Bellows, D. Jia, Y. Jia, A. Hassanloo, J.N. Heersche, Different effects of insulin and insulin-like growth factors I and II on osteoprogenitors and adipocyte progenitors in fetal rat bone cell populations, Calcif. Tissue Int. 79 (2006) 57–65.
[32] B. de Crombrugghe, Osteoblasts clock in for their day job, Cell 122 (2005) 651–653.
[33] B. Lecka-Czernik, C.J. Rosen, Skeletal integration of energy homeostasis: translational implications, Bone 82 (2016) 35–41.
[36] A. Sainsbury, C. Schwarzer, M. Couzens, H. Herzog, Y2 receptor deletion attenuates the type 2 diabetic syndrome of ob/ob mice, Diabetes 51 (2002) 3420–3427.
[37] N.J. Lee, I.P. Wong, P.A. Baldock, H. Herzog, Leptin as an endocrine signal in bone, Curr. Osteoporos. Rep. 6 (2008) 62–66.
[38] H. Wise, The roles played by highly truncated splice variants of G protein-coupled receptors, J. Mol. Signal. 7 (2012) 13.
[39] S. Majumdar, S. Grinnell, V. Le Rouzic, M. Burgman, L. Polikar, M. Ansonoff, J. Pintar, Y.X. Pan, G.W. Pasternak, Truncated G protein-coupled mu opioid receptor MOR-1 splice variants are targets for highly potent opioid analgesics lacking side effects, Proc. Natl. Acad. Sci. U. S. A. 108 (2011) 19778–19783.
[40] M. Duran-Prado, M.D. Gahete, A.J. Martinez-Fuentes, R.M. Luque, A. Quintero, S.M. Webb, P. Benito-Lopez, A. Leal, S. Schulz, F. Gracia-Navarro, M.M. Malagon, J.P. Castano, Identification and characterization of two novel truncated but functional isoforms of the somatostatin receptor subtype 5 differentially present in pituitary tumors, J. Clin. Endocrinol. Metab. 94 (2009) 2634–2643.